

# Critical Current Oscillations in Strong Ferromagnetic Pi-Junctions

J. W. A. Robinson<sup>1</sup>, S. Piano<sup>1,2</sup>, G. Burnell<sup>1</sup>, C. Bell<sup>3</sup>, and M. G. Blamire<sup>1</sup>

1. Department of Material Science, University of Cambridge, Pembroke Street, Cambridge CB2 3QZ, UK  
 2. Physics Department, CNR-Supermat Laboratory, University of Salerno, Via S. Allende, 84081 Baronissi (SA), Italy  
 3. Kamerlingh Onnes Laboratory, Leiden University, P.O. Box 9504, 2300 RA Leiden, The Netherlands

(Dated: 21 July 2006)

We report magnetic and electrical measurements of Nb Josephson junctions with strongly ferromagnetic barriers of Co, Ni and Ni<sub>80</sub>Fe<sub>20</sub> (Py). All these materials show multiple oscillations of critical current with barrier thickness implying repeated 0- $\pi$  phase-transitions in the superconducting order parameter. We show in particular that the Co barrier devices can be accurately modelled using existing clean limit theories and so that, despite the high exchange energy (309 meV), the large  $I_c R_N$  value in the  $\pi$ -state means Co barriers are ideally suited to the practical development of superconducting  $\pi$ -shift devices.

PACS numbers: 74.50.+r, 74.25.5V, 74.78.Db, 74.25.Ha.

Although the interplay of superconductivity and ferromagnetism has been the subject of study for many decades [1], theoretical and experimental investigations into the properties of superconductor-ferromagnetic metal (S/F) heterostructures have seen an upsurge in interest in recent years following the experimental observation of 0 to  $\pi$  transitions in the superconducting order parameter in S/F thin films by Ryzhanov *et al.* [2] and by Kontos *et al.* [3]. In terms of the Josephson relationship  $I_c = I_0 \sin \Delta\phi$ , where  $\Delta\phi$  is the phase difference between the two S layers, a transition from the 0 to  $\pi$  states implies a change in sign of  $I_0$  from positive to negative. Physically, such a change in sign of  $I_0$  is a consequence of a phase change in the electron pair wave function induced in the F layer by the proximity effect. Experimentally, measurements of  $I_c$  are insensitive to the sign of  $I_0$  and hence the absolute  $I_c$  is measured; this implies that a change in state from 0 to  $\pi$  will lead to a zero crossing of  $I_c$  and a sharp cusp at  $I_c = 0$ . It is possible to describe the  $I_c$  dependence with ferromagnetic thickness ( $d_F$ ) by the generic expression

$$I_c R_N(d_F) \propto I_c R_N(d_0) \left| \frac{\sin \frac{d_F - d_1}{\xi_2}}{\sin \frac{d_F - d_0}{\xi_1}} \right| \exp \left\{ \frac{d_0 - d_F}{\xi_1} \right\}, \quad (1)$$

where  $d_1$  is the thickness of the ferromagnet corresponding to the first minimum and  $I_c R_N(d_0)$  is the first experimental value of  $I_c R_N$  ( $R_N$  is the normal state resistance). Transitions can be observed as oscillations in the critical temperature ( $T_c$ ) of S/F multilayers [4, 5, 6, 7] as well as oscillations in the  $I_c$  of S/F/S junctions with both thickness of the F layer [8, 9, 10] and, for weak ferromagnets whose exchange energy ( $E_{ex}$ ) is comparable to  $k_B T_c$  of the superconductor, with temperature [11].

The majority of studies of S/F/S structures have concentrated on the use of weak ferromagnets, such as Cu<sub>x</sub>Ni<sub>1-x</sub> and Pd<sub>x</sub>Ni<sub>1-x</sub>, where the temperature dependence can be observed and where thickness of the ferromagnetic layer over which oscillations in critical temperature or current are observed can be comparatively large. Even where strong ferromagnets have been used, a significant magnetic ‘dead’ layer corresponding to a loss in total moment [12] is usually observed which complicates the modeling - see table I.

In the dirty limit where the mean free path  $L < d_F$  and  $L < \hbar v_f / E_{ex}$  the two decay lengths,  $\xi_1$  and  $\xi_2$ , take similar values and so multiple oscillations of  $I_c$  are not observed. In contrast, in the clean limit where  $d_F < L$  and  $L > \hbar v_f / E_{ex}$  the decay of the envelope determining the modulation amplitude ( $\xi_1$ ) can be much larger than the oscillation period ( $\xi_2$ ). Most previous studies, including those using strong ferromagnets, have been performed in the dirty limit; for practical applications, in which large  $I_c R_N$  values are required in the  $\pi$  state it is vital to develop high quality clean limit S/F/S devices. A recent report using the ferromagnetic intermetallic Ni<sub>3</sub>Al shows  $I_c$  oscillations in the clean limit [13], but with a very large magnetic dead layer which is not accounted for in any phenomenological model and which is likely to make practical control of the phase state of the junction difficult.

Co is a proven device material which can be deposited in clean thin film form with accurately controlled thickness; however, it has not been previously applied in S/F/S junctions because the exchange energy was considered to be far too large. In this letter, we report for the first time measurements of junctions containing Co barriers, together with comparative studies of Py and Ni barriers. We show that, unlike Py and Ni and the weak ferromagnets, the Co data fits excellently to clean limit theory. As importantly, the magnetic dead layer in the Co is less than 1 nm allowing precise control of the phase state of Nb/Co/Nb  $\pi$ -junctions.

Nb/Co/Nb, Nb/Py/Nb and Nb/Ni/Nb films were deposited on 10 × 5 mm silicon (100) substrates coated with a 250 nm thermal oxide. Simultaneously to growing 10 × 5 mm thin films for patterning, identical 5 × 5 mm films were deposited for magnetic characterization in a vibrating sample magnetometer (VSM). All of the layers were deposited by d.c. magnetron sputtering at 1.5 Pa and the deposition system was baked out for seven hours and subsequently cooled with liquid nitrogen for at least one hour prior to the deposition, which gave a base pressure better than  $5 \times 10^{-6}$  Pa and an oxygen partial pressure of less than  $3 \times 10^{-9}$  Pa. The deposition rates are:  $1.2 \text{ nm min}^{-1}$  for Co,  $1.6 \text{ nm min}^{-1}$  for Py,  $0.4 \text{ nm min}^{-1}$  for Ni,  $2.4 \text{ nm min}^{-1}$  for Cu and  $12.6 \text{ nm min}^{-1}$  for Nb. In a single deposition run, multiple silicon substrates were placed on a rotating holder which

passed in turn under three magnetrons. The thickness of each layer was controlled by setting the angular speed at which the substrates moved under the respective targets and by setting the target power. When depositing Co, Py, and Ni barriers, an acceleration curve was programmed which allowed the angular speed of the substrates to change monotonically as the substrates passed under the relevant targets. The thickness of the Co ( $d_{Co}$ ), Py ( $d_{Py}$ ) and Ni ( $d_{Ni}$ ) was then dependent on the substrate position,  $\theta$ , on the rotating holder. With knowledge of the deposition parameters, the rotation was programmed such that  $d(d_F)/d\theta$  was a constant. This method of varying  $d_F$  guaranteed in all cases that the interfaces between each layer prepared under the same conditions and the only variation was the thickness. To confirm control over the thicknesses we performed X-ray reflectivity of Nb/Co/Nb thin films where the Nb layers had a thickness of 5 nm and the Co barrier thickness was varied from 0.5 nm to 5.0 nm. A series of low angle X-ray scans were made and the thickness of the Co layer ( $d_{Co(observed)}$ ) extracted by fitting the period of the Kiessig fringes using a simulation package. It was found that our expected thicknesses,  $d_{Co(expected)}$ , was well correlated with  $d_{Co(observed)}$  with a mean deviation of 0.2 nm.

To assist in locating the barrier layer in subsequent focused ion beam (FIB) processing, a thin (20 nm) normal metal layer of Cu was embedded in the 250 nm thick Nb electrodes located 50 nm from the ferromagnetic layer (a distance greater than the coherence length of Nb). At 20 nm, the Cu layer is much thinner than the coherence length in Cu and is therefore totally proximitised by the Nb and plays no part in the electrical properties of the junctions. The thicknesses of the F barriers for the Co and Py junctions was varied from approximately 0.5 nm to 5 nm and the Ni barrier thickness was varied from 1.0 nm to 10 nm. The films were patterned using optical lithography, followed by broad beam Ar ion milling ( $3 \text{ mA cm}^{-2}$ , 500 V beam) to produce micron scale tracks and contact pads, to allow four-point measurements to be performed. These tracks were then patterned with a  $\text{Ga}^+$  FIB (Philips/FEI FIB 200) to achieve vertical transport with a device area in the  $0.2 - 1 \mu\text{m}^2$  range. The FIB technique for processing such junctions is described in detail elsewhere [14]. A micrograph of one of the junctions processed using the FIB for this work is shown as the inset of Fig. 2(a).

To investigate the magnetic properties of our films we have measured, using a VSM at room temperature, the magnetic moment per unit surface area of the films as a function of  $d_F$  (see Fig. 1). Extrapolating the least-squares fit of the data in Fig. 1 gives magnetic dead layers of  $\simeq 0.75 \text{ nm}$  for Co,  $\simeq 0.5 \text{ nm}$  for Py and  $\simeq 1.5 \text{ nm}$  for Ni. The causes of a magnetic dead layer are attributed to factors such as lattice mismatch causing elastic deformation, formation of amorphous interfaces and a breakdown in the crystal structure leading to a reduced exchange interaction between neighbouring atoms and hence a reduction in  $T_{Curie}$  and  $E_{ex}$  [15, 16, 17]. In the case of Co and Ni, both the thickness of the dead layer and the total moments for a given thickness greater than the dead layer are close to those reported in systematic studies Nb/F bilayers

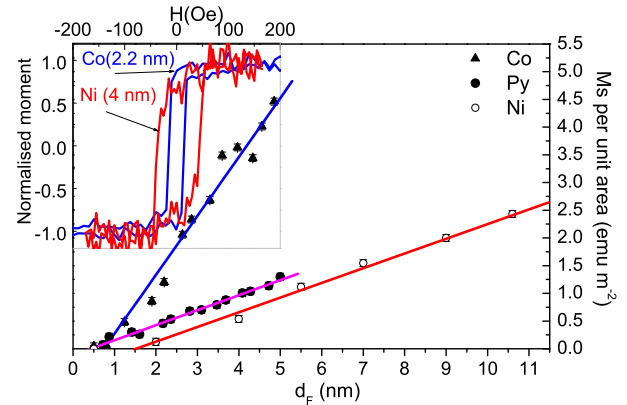


FIG. 1: (Color online) Scaling of the magnetic moment per unit area vs. Co, Py and Ni barrier thickness at room temperature. Inset: hysteresis loops for Co and Ni at room temperature.

[6, 18].

Transport measurements were made in a liquid He dip probe. The differential resistance as a function of bias current of the junctions was measured with a standard lock-in technique. The  $I_c$  was found from the differential resistance as the point where the differential resistance increases above the value for zero bias current.  $R_N$  was measured using a quasi-dc bias current of 3-5 mA, this enabled the nonlinear portion of the I-V curves to be neglected, but was not large enough to drive the Nb electrodes into a normal state. A  $dV/dI(I)$  and  $V(I)$  plot for a typical Nb-Py-Nb Josephson junction is shown inset of Fig. 2(b). In general, the critical currents of the devices measured for this work ranged from  $500 \mu\text{A}$  to below the minimum sensitivity of our apparatus ( $50 \text{ nA}$ ), while the normal state resistances were in the range  $1.0 \text{ m}\Omega$  to  $100 \text{ m}\Omega$ .

The variation of  $I_c R_N$  as a function of Co, Py and Ni thickness at 4.2 K is shown in Figs. 2(a-c) respectively. Each point in these Figs. corresponds to the mean of several junctions with different areas; the vertical error bars are derived from the measured variation in  $I_c R_N$  and a small noise contribution due to the current source. From X-ray reflectivity results, as discussed above, we take the error in  $d_F$  for all F barriers to be  $\approx 0.2 \text{ nm}$ . All of the devices shown in this data set presented Shapiro steps upon the application of microwaves and an  $I_c$  modulation with applied field  $H_A$ . For the devices where  $d_{Co} > 5 \text{ nm}$ ,  $d_{Py} > 5 \text{ nm}$ , and  $d_{Ni} > 13 \text{ nm}$  some reduction of the differential resistance around  $I = 0$  was seen, but did not show a measurable supercurrent at 4.2 K. As expected,  $I_c R_N$  for the Co, Py and Ni decreases exponentially and in an oscillatory fashion with  $d_F$ .

The Co data was modeled using Eq. (1); from the model fit shown in Fig. 2(a) we find that the period of the Co oscillations is  $\simeq 1.9 \text{ nm}$ , hence  $\xi_2 \simeq 0.3 \text{ nm}$  and  $\xi_1 \simeq 3.0 \text{ nm}$ . This gives a  $\xi_2/\xi_1$  ratio of  $\sim 0.11$ . A full theoretical treatment involves solving linear Eilenberger equations [19] and gives Eq. (2)

$$\tanh \frac{L}{\xi_{eff}} = \frac{\xi_{eff}^{-1}}{\xi_0^{-1} + L^{-1} + i\xi_H^{-1}} \quad (2)$$

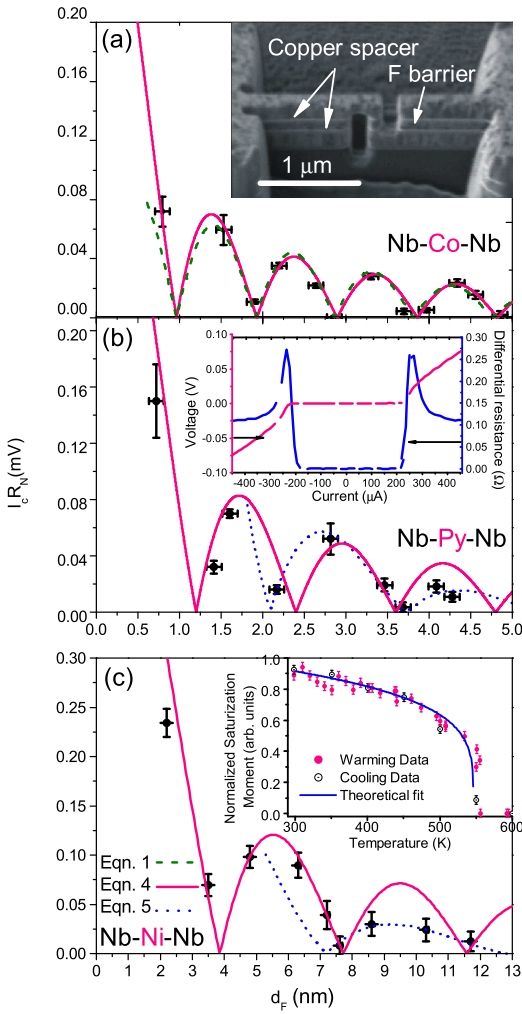


FIG. 2: (Color online) Characteristic voltage as a function of Co, Py and Ni thickness at 4.2K. The solid lines are fits to Eq. (4), the dotted lines are fits to Eq. (5), and the dashed line is a fit to Eq. (1) as described in text. Inset (a): An FIB micrograph of a typical Nb-Co-Nb Josephson junction. Inset (b):  $V(I)$  and  $dV/dI(I)$  plotted for a Nb/Py/Nb Josephson junction at 4.2K. Inset (c): normalised magnetization as a function of warming and cooling temperature for a Nb/Ni/Nb trilayer where  $d_{Ni} \simeq 9$  nm.

where  $\xi_{eff}$  is the effective decay length given by  $\xi_{eff}^{-1} = \xi_1^{-1} + i\xi_2^{-1}$ ,  $\xi_0$  is the Ginzburg-Landau coherence length and  $\xi_H$  is a complex coherence length. In the clean limit  $1 + L\xi_0^{-1} \gg \frac{1}{2} \max\{\ln(1 + L\xi_0^{-1}), \ln(L\xi_H^{-1})\}$ . The solution of Eq. (2) gives

$$\xi_1^{-1} = \xi_0^{-1} + L^{-1}, \xi_0 = \frac{v_F \hbar}{2\pi T_c k_B}, \xi_2 = \xi_H = \frac{v_F \hbar}{2E_{ex}}, \quad (3)$$

and the numerical solution is shown in Fig. (3).

Following the method of Gusakova and Kupriyanov [19] we find from Fig. (3) that the experimental ratio  $\xi_2/\xi_1 \simeq 0.1$  corresponds to two inverse magnetic lengths of  $L/\xi_H \simeq 16.5$  and  $L/\xi_H \simeq 18.7$ . By assuming  $L/\xi_0 \simeq 0.1$  and for the estimated parameters  $\xi_1 \simeq 3$  nm and  $\xi_2 \simeq 0.3$  nm we obtained, from the inset in Fig. (3) that for  $L/\xi_H \simeq 16.5$

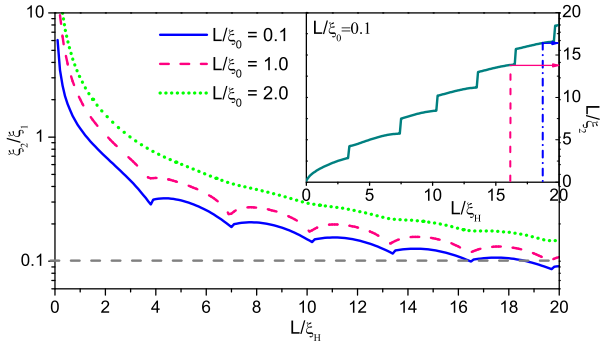


FIG. 3: (Color online) The dependence of  $\xi_2/\xi_1$  with inverse magnetic length,  $L/\xi_H$ , calculated for different ratios of  $L/\xi_0$ . Inset: inverse decay length,  $L/\xi_2 = f(L/\xi_H)$  for when  $L/\xi_H \simeq 0.1$

and  $L/\xi_H \simeq 18.7$ ,  $\bar{L} \simeq 5$  nm. Inputting these values into Eq. (3) gives  $v_F(Co) \simeq 2.8 \times 10^5$  ms<sup>-1</sup> which is similar to other reported values of  $v_F(Co)$  [20] and  $E_{ex} \simeq 309$  meV. To validate the mean free path of our Co thin film we have estimated  $L(Co)$  in a 50 nm thick Co film by measuring its resistivity as a function of temperature using the Van der Pauw technique [21]. Following the method described by Gurney *et al.* we estimate that our Co has a mean free path of  $L(Co) \simeq 10$  nm which justifies our assumption of a clean limit fit. As a comparison we have also modeled the Co oscillations with a simpler theoretical model given by Eq. (4) [23]

$$I_C R_N \propto \frac{|\sin(2E_{ex}d_F/\hbar v_f)|}{2E_{ex}d_F/\hbar v_f}. \quad (4)$$

As in the case of Eq. (1) the fitting between the theoretical model and the experimental data is good (see Fig. 2 (a) dashed line) and in particular the best fitting has been obtained by using  $v_F = 2.8 \times 10^5$  ms<sup>-1</sup> and  $E_{ex} = 309$  meV.

In contrast, the Py and Ni data cannot be fitted entirely in the clean limit. In the case of Py, Eq. (4), closely matches the experimental data up to a thickness of  $\simeq 3.6$  nm and in the case of Ni the oscillations follow the clean limit theory to  $\simeq 7$  nm. Above these values a better fit is obtained using a formula for a diffusive and high  $E_{ex}$  F [24]:

$$I_C R_N \propto |Re \sum_{\omega_m > 0} \frac{\Delta^2}{\Delta^2 + \omega_m^2} \int_{-1}^1 \frac{\mu}{\sinh(k_\omega d_F/\mu L)} d\mu|, \quad (5)$$

where  $\Delta$  is the superconducting energy gap,  $\omega_m$  is the Mat-subara frequency and is given by  $\omega_m = \pi T k_B (2m+1)$  where  $T$  is the transmission coefficient and  $m$  is an integer number.  $k_\omega = (1 + 2 |\omega_m| \tau/\hbar) - 2iE_{ex}\tau/\hbar$  and  $\mu = \cos \theta$  where  $\theta$  is the angle the momentum vector makes relative to the distance normal to the SF interface.  $L$  is given by  $v_f \tau$  and  $\tau$  is the momentum relaxation time. For Eq. (4) the only fitting factor, besides the numerical prefactor, was the strength of the exchange interaction ( $E_{ex}/\hbar v_f$ ). In the case of Eq. (5) a suitable  $v_f$ ,  $\Delta$  and  $E_{ex}$  had to be chosen. To fit Eq. (5) to Py and Ni data we used:  $v_f(Py) = 2.2 \times 10^5$  m/s and  $L_{Py} \simeq 2.3$  nm, and  $v_f(Ni) = 2.8 \times 10^5$  m/s and  $L_{Ni} \simeq 7$  nm and  $\Delta = 1.3$

$\xi_1$ (nm)	$\xi_2$ (nm)	F	$v_F$ (ms $^{-1}$ )	$E_{ex}$ (meV)	DL(nm)	Ref
1.2	1.6	Ni <sub>20</sub> Fe <sub>80</sub>	$2.2 \times 10^5$	95	0.7	[9]
1.4	0.46	Ni <sub>20</sub> Fe <sub>80</sub>	$2.2 \times 10^5$	201	0.5	*
1.8	2.0	Pd <sub>90</sub> Ni <sub>10</sub>	$2.0 \times 10^5$	35	-	[3]
1.7	1.0	Ni	$2.8 \times 10^5$	200	-	[10]
2.3	0.86	Ni	$2.8 \times 10^5$	107	-	[8]
4.1	1.2	Ni	$2.8 \times 10^5$	80	1.5	*
4.6	0.45	Ni <sub>3</sub> Al	$1.5 \times 10^5$	86	5-8	[13]
3.0	0.3	Co	$2.8 \times 10^5$	309	0.8	*

TABLE I: A summary of reported parameters for different material systems. DL stands for ‘Dead Layer Thickness’ and \* ‘This paper’.

meV. These values are consistent with the ones used in Eq. (4) and elsewhere [8, 9]. From the oscillations period we can estimate the  $E_{ex}$  of the Py and Ni barriers - from Eq. (4) the periodicity is given by  $L_{osc} \sim \hbar v_f / 2E_{ex}$  and hence we can deduce  $E_{ex}$ . The exchange energies for Py and Ni were found to be 201 meV and 80 meV respectively.  $E_{ex}(Py)$  is approximately double that measured in Nb/Py/Nb junctions deposited with epitaxial barriers where  $E_{ex}$  was found to be 95 meV [9].  $E_{ex}(Ni)$  is close to other reported values by photoemission experiments [26]. The smaller than expected  $E_{ex}$  is a consequence of impurities and possibly interdiffusion of Ni into Nb. In the case of Ni, we have measured the magnetisation saturation as a function of temperature ( $M(T)$ ) (see inset of Fig. 2(c)) so that an estimate of the Ni Curie temperature could be made. This provides further evidence that our Ni data is consistent and that the Ni isn’t grossly degraded. To be sure our data was not influenced by thermal diffusion during this measurement we measured  $M(T)$  for both the heating and cooling phases and it is shown that the cooling curve follows the warming one. The warming data is modeled by the formula:  $M(T)/M(0) = (1 - T/T_{Curie})^\beta$  where  $M(0)$  is the magnetisation at absolute 0 K,  $T$  is the measuring temperature, and  $\beta$  and  $T_{Curie}$  are fitting parameters. We estimate  $T_{Curie} \simeq 571$  K which is in agreement with Curie temperature measurements of Ni in S/F bilayers [25].

The fully clean limit behavior observed with the Co barriers arises most obviously from the use of a pure element, but also from the vertical coherence likely [27] even in noncrystalline heterostructures. The high  $E_{ex}$  results in a short oscillation period implying a need for Å-level control of layer thickness for practical devices; however Co and Co-alloys form the basis of current spintronic device production, and precision layer control and excellent compatibility with tunnel barriers [28] have been demonstrated in many industrial processes [29]. Co is an attractive material for qubits and other novel devices.

In summary, we have measured critical current oscillations in Co junctions as a function of Co barrier thickness which indicates that the devices are strongly in the clean limit. This results in a higher  $I_c R_N$  values in the  $\pi$  state compared to  $I_c R_N$  values in the dirty limit. We also present complementary critical current oscillations through Py and Ni barriers.

The oscillations in  $I_c R_N$  with  $d_F$  are indicative of 0 –  $\pi$  crossovers, but without conducting phase-sensitive measurements the specific phases of the individual junctions cannot be known. The oscillations also showed an excellent fit to theoretical models. We have also estimated, from the periodicity of the oscillations, the exchange energies of the Co, Py and Ni barriers to be 309 meV, 201 meV and 80 meV respectively. Results within this paper are summarized in table I alongside results reported elsewhere. Our results are not only interesting in their own right, but are a vital experimental step towards understanding the physics of quantum electronic devices based on superconductors and are of considerable value to the development of quantum information processing. Our devices are precursors to practical implementations into qubits and other applications in controllable and scalable superconducting quantum electronic devices.

The authors thank M. Yu. Kupriyanov, A. M. Cucolo, and F. Bobba for helpful discussions and N. Stelmashenko for technical assistance. We acknowledge the support of the EPSRC UK and the European Science Foundation  $\pi$ -shift network.

---

- [1] A. I. Buzdin, Rev. Mod. Phys. **77**, 935 (2005).
- [2] V. V. Ryazanov *et al.*, Phys. Rev. Lett. **86**, 2427 (2001).
- [3] T. Kontos *et al.*, Phys. Rev. Lett. **89**, 137007 (2002).
- [4] J. S. Jiang *et al.*, Phys. Rev. Lett. **74**, 314 (1995).
- [5] Th. Mühge *et al.*, Phys. Rev. Lett. **77**, 1857 (1996).
- [6] Y. Obi *et al.*, Physica C **317-318**, 149 (1999).
- [7] L. Lazar *et al.*, Phys. Rev. B **61**, 3711 (2000).
- [8] Y. Blum *et al.*, Phys. Rev. Lett. **89**, 187004-1 (2002).
- [9] C. Bell *et al.*, Phys. Rev. B **71**, 180501(R) (2005).
- [10] V. Shelukhin *et al.*, cond-mat/0512593 (2006).
- [11] H. Sellier *et al.*, Phys. Rev. B **68**, 054531 (2003).
- [12] S. Pick *et al.*, St. Commun. **124**, 21 (2002).
- [13] F. Born *et al.*, cond-mat/0604277 (2006).
- [14] C. Bell *et al.*, Nanotechnology **14**, 630 (2003).
- [15] J. Aarts *et al.*, Phys. Rev. B **56**, 2779 (1997).
- [16] R. Zhang and R. F. Willis, Phys. Rev. Lett. **86**, 2665 (2001).
- [17] Q. Leng *et al.*, J. Appl. Phys. **87**, 6621 (2000).
- [18] J. E. Mattson, R. M. Osgood, C. D. Potter, C. H. Sowers, and S. D. Bader, J. Vac. Sci. Technol. A, **15**, 1774 (1997).
- [19] D. Yu. Gusakova, M. Yu. Kupriyanov and A. A. Golubov, cond-mat/0605137 (2006).
- [20] D. Y. Petrovykh *et al.*, Appl. Phys. Lett. **73**, 23 (1998).
- [21] B.A. Gurney *et al.*, Phys. Rev. Lett. **71**, 4023 (1993).
- [22] J. Kötzler and W. Gil, Phys. Rev. B **72**, 060412(R) (2005).
- [23] A. I. Buzdin, JETP Lett. **35**, 178 (1982).
- [24] F. S. Bergeret *et al.* Phys. Rev. B **(64)**, 134506 (2001).
- [25] J. Kim, J. H. Kwon, K. Char, H. Doh, and H. Y. Choi, Phys. Rev. B **72** 014518 (2005).
- [26] P. Heinmann, F.J. Himpsel, and D.E. Eastman, Solid State Comm. **39**, 219 (1981).
- [27] C. W. Leung *et al.*, J. Mag. Mag. Mats. **269** (1), 15 (2004).
- [28] I. I. Oleinik *et al.*, Phys. Rev. B **62**, 3952 (2000).
- [29] C. Kaiser and S. S. P. Parkin, Appl. Phys. Lett., **84**, 3582 (2004)